Safety in Extreme Environments (2023) 5:253–263
https://doi.org/10.1007/s42797-023-00082-8

RESEARCH

A novel Schiff base of pyridine-2-amine derivative as an effective inhibitor of the dissolution of N80 pipeline steel in 1 M HCl

Nkem B. Iroha[1] · **Cordelia U. Dueke-Eze**[2]

Received: 9 March 2023 / Revised: 10 July 2023 / Accepted: 19 July 2023 / Published online: 25 July 2023

Abstract
An investigation of the performance of recently synthesized pyridine-2-amine derivative namely, N-(5-methoxy-2-hydroxybenzylidene)pyridine-2-amine (N5MHP) as inhibitor of N80 steel corrosion in 1 M HCl environment was carried out using surface analysis, electrochemical impedance, polarization and weight loss method. Results obtained reveal that N5MHP performed well in protecting the steel surface, achieving an inhibition efficiency of 97.0% at 303 K with 1.0 mM concentration from weight loss method. Increasing temperature depreciated the corrosion inhibition efficiency of N5MHP but increase in concentration enhanced the protection performance of the inhibitor. Electrochemical tests results agreed with weight loss results. Langmuir isotherm was obeyed by N5MHP in its adsorption on the steel surface. Polarization studies revealed that N5MHP acted as mixed-type inhibitor. Surface morphology characterized using scanning electron microscopy (SEM) displayed a more protected surface of the X60 steel in the presence of N5MHP in the acid media. Theoretical calculations were performed by employing Density Functional Theory (DFT).

Keywords Pyridine-2-amine · N80 steel · Electrochemical impedance · Langmuir isotherm · Corrosion inhibition · DFT calculations

Introduction

Corrosion creates different serious problems in various industries due to its precarious and damaging effect on metals. It is one of the main causes of structural deterioration in offshore and marine structures (Anwar et al. 2019, 2021). Cleaning of pipework steel in order to remove undesirable rust and scale is usually done with acid solutions like hydrochloric acid which subjects the steel to corrosion (Abd-Elaal et al. 2013). In acid solutions, apart from metal dissolution (anodic process) corrosion is usually accompanied by cathodic processes which predominantly involve hydrogen gas evolution. The study of steel corrosion in acid media has been of interest to researchers due to increased applications of acid solution. Pipework steel protection with corrosion inhibitors has greatly been investigated and found to be one of the most desirable corrosion prevention methods (Njoku et al. 2021; Iroha and Nnanna 2021; Kousar et al. 2021). These inhibitors are chemicals usually added in small quantity to the corrosive environments to slowdown the corrosion rate (Iroha and James 2019). Several organic compounds (Arrousse et al. 2021; Kacimi et al. 2017; Poojary et al. 2021; Iroha et al. 2005) have been applied as inhibitors for steel corrosion in acidic media and found to be effective in reducing the corrosion rate. These compounds exert inhibitive action by adsorption of their molecules onto the steel surface, thereby creating a protective barrier to attack of the corrodant. Based on extensive study, the organic compounds are able to adsorb effectively on the metal surface most likely because of the presence of multiple bonds, aromatic rings, heterocyclic and, N, O, S and P atoms present in their molecules. These atoms contain electron lone pairs which are available to the iron empty d-orbital to form a dative bond.

Schiff bases with general formula RC = NR′ have in their structure, features that make them potent as corrosion inhibitors. Schiff bases are compounds produced by the condensation of amines and a carbonyl compound. The ease of synthesis of these compounds from affordable materials is one

✉ Nkem B. Iroha
irohanb@fuotuoke.edu.ng

[1] Electrochemistry and Material Science Unit, Department of Chemistry, Federal University Otuoke, P.M.B. 126, Yenagoa, Bayelsa State, Nigeria

[2] Chemistry Department, University of Lagos, Akoka, Lagos State, Nigeria

the great advantages of Schiff bases in their use as corrosion inhibitors. Recent reports have shown the effectiveness of Schiff bases as inhibitors of steel corrosion in acid media (Yurt et al. 2014; Okey et al. 2020). Literature survey has also revealed the use of Schiff bases derived from pyridine as corrosion inhibitors (Ansari et al. 2015; Iroha et al. 2021). This synthesized pyridine derivative is a non-toxic organic compound which is also useful and important intermediate in various medicinal compounds preparations (Cocco et al. 2003; Hughes et al. 2008). This type of Schiff base contains heterocyclic compounds with nitrogen atoms which can be protonated easily in acidic environment to display effective inhibition of metals corrosion in acid solution.

In an attempt to contribute to this research area which is growing and solving industry problems, we have in our laboratory, synthesized and used some Schiff bases (Dueke Eze et al. 2022; Iroha and Dueke-Eze 2021) which have performed well as corrosion inhibitors. This present work is aimed at studying the inhibitory performance of Schiff base N5MHP on the corrosion of N80 steel in 1 M HCl environment using electrochemical and weight loss techniques. This compound was chosen on the basis of molecular structure, while considering the active centers and the kind of substituents. To correlate the inhibition performance of N5MHP with its structure, quantum chemical calculations were performed.

Experimental

Preparation of metal specimen and corrosion medium

The metal specimens (N80 steel) used for the study contained; 0.92% Mn, 0.01% P, 0.31% C, 0.008% S, 0.19% Si, 0.2% Cr and the remainder Fe. The steel specimens were first cut into 2×4 cm^2 dimensions for both weight loss and electrochemical measurements and then abraded with emery papers (grades 400–1200). The specimens were thereafter rinsed with distilled water, dried in an oven after degreasing with acetone and then utilize for the experiment. Exposed area of 1 cm^2 for the samples was utilized in electrochemical studies. The blank corrosion medium consists of 1 M HCl solution prepared from analytical grade 37% HCl (Merck) by diluting with distilled water.

Synthesis of N5MHP

5-methoxy-2-hydroxybenzaldehyde solution (24.5 mg, 0.20 mmol) in 10 mL of ethanol and formic acid (two drops) were mixed with 2-aminopyridine solution (18.8 mg, 0.20 mmol) in 10 mL of ethanol and stirred. For 6 h the mixture was refluxed and the precipitate formed was filtered and then recrystallized to yield N-(5-methoxy-2-hydroxybenzylidene) pyridine-2-amine (N5MHP). Detailed characterization by NMR and IR has been earlier reported (Dueke-Eze et al. 2013). The molecular structure of N5MHP is shown in Fig. 1.

Electrochemical measurements

Electrochemical measurements were perform by utilizing the conventional three-electrode electrolytic cell with N80 steel as working electrode, platinum foil as counter electrode and saturated calomel electrode (SCE) [$Hg/Hg_2Cl_2/KClsat$] as reference electrode. All measurements were performed using Gamry framework at 30 °C. Samples were mounted in epoxy resin with an exposed area of 1 cm^2 to the test solution. The experiment proceeded by first letting the working electrode attain a steady state via immersion in the test solution for 30 min at open circuit potential (OCP). The electrochemical impedance spectroscopy (EIS) measurement performed on the N80 steel electrode at OCP proceeded by applying a signal amplitude of 10 mV within the range of frequency 100 kHz to 0.01 Hz. Fitting and analyses of the EIS data were done with Echem Analyst software version 5.50. The polarization measurement were performed from potential (cathodic) of -0.25 V vs. OCP to potential (anodic) of +0.25 V vs. OCP at a scan rate 1 mVs^{-1}. Results reproducibility was tested by repeating the measurements three times.

Weight loss measurement

The weight loss measurements were conducted using ASTM G31-72 standard (ASTM 2004). In this measurement, the N80 steel specimens were weighed and suspended in solutions containing 100 mL bare 1 M HCl and different concentrations of N5MHP for 6 h immersion time at 30 °C, 40 and 50 °C temperatures unstirred. The N80 steel specimens were retrieved washed, dried and accurately re-weighed. The average of three weight loss measurements was recorded. The corrosion rate (C_R), surface coverage (θ) and inhibition efficiency (IE_{WL} %) for N5MHP were respectively computed using Eqs. 1, 2 and 3:

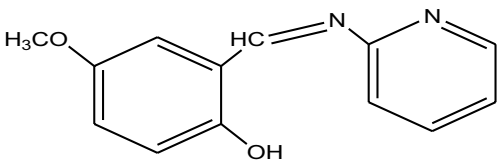

Fig. 1 Molecular structure of N5MHP

$$C_R = \frac{\Delta W}{S.t} \quad (1)$$

where ΔW represents mean weight loss (mg), t and S stand for immersion time (s) and surface area (cm^2) respectively.

$$\theta = \frac{C_R - C_{R(i)}}{C_R} \quad (2)$$

$$IE_{WL}\% = \frac{C_R - C_{R(i)}}{C_R} \times 100 \quad (3)$$

where C_R and $C_{R(i)}$ are corrosion rate values of X60 steel without and with the inhibitors respectively.

SEM analysis

SEM micrographs of the N80 steel specimen immersed in blank 1 M HCl and inhibited with 1×10^{-2} M N5MHP were examined utilizing Ziess Evo 50 XVP model of scanning electron microscope. The SEM operating at 20 kV recorded the topography of the surface with resolution of electron microscope of 1.5 nm. The SEM images were taken at 2000× magnification. After 6 h immersion at 30 °C, the specimens were retrieved from the test solutions, washed properly with distilled water and dried in air before SEM analysis.

Quantum Chemical Calculations

The quantum chemical calculations were performed using Spartan 14.0 software. The calculations and geometrical optimization of N5MHP inhibitor were carried out utilizing the B3LYP model of density functional theory (DFT) in combination with the 6-311G (d, p) basis sets. The HOMO energy (E_{HOMO}), LUMO energy (E_{LUMO}) and the energy gap ($\Delta E = E_{LUMO} - E_{HOMO}$) were calculated to determine the inhibition behavior of N5MHP. The calculated E_{HOMO} and E_{LUMO} were used to calculate some important parameters like electron affinity ($EA = -E_{LUMO}$), ionization potential ($IP = -E_{HOMO}$) and other such as electronegativity (χ), global hardness (η) and global softness (σ) as shown in Eqs. (4)–(6) (Zhang et al. 2015; Iroha et al. 2022a):

$$\chi = \frac{IE + EA}{2} \quad (4)$$

$$\eta = \frac{IP - EA}{2} \quad (5)$$

$$\sigma = \frac{1}{\eta} \quad (6)$$

The change in the number of transported electrons (ΔN) from the inhibitors to the Fe surface was calculated by Eq. (7) (Xia et al. 2015; Maduelosi and Iroha 2020):

$$\Delta N = \frac{\chi_{Fe} - \chi_{inh}}{2(\eta_{Fe} + \eta_{inh})} \quad (7)$$

where χ_{Fe} and χ_{inh} are the electronegativity of Fe and inhibitor molecules, while η_{Fe} and η_{inh} are the global hardness of Fe and inhibitor molecules. From Pearson's electronegativity scale, the theoretical values of η_{Fe} and χ_{Fe} are 0 eV and 7 eV (Zhang et al. 2019).

Results and discussion

Potentiodynamic polarization measurements (PDP)

A potentiodynamic polarization test was carried out to gain insight into the kinetics of the anodic and cathodic reactions. The anodic reaction involves N80 steel dissolution through oxidation process as earlier described (Hamani et al. 2014; Iroha et al. 2022b):

$$Fe + Cl^- \rightleftharpoons (FeCl^-)_{ads} \quad (8)$$

$$(FeCl^-)_{ads} \rightleftharpoons (FeCl)_{ads} + e^- \quad (9)$$

$$(FeCl)_{ads} \rightarrow (FeCl)^+ + e^- \quad (10)$$

$$(FeCl)^+ \rightleftharpoons Fe^{2+} + Cl^- \quad (11)$$

While on the contrary, the cathodic reaction has to do with the hydrogen evolution through reduction process as follows described (Hamani et al. 2014; Iroha et al. 2022b):

$$Fe + H^+ \rightleftharpoons (FeH^+)_{ads} \quad (12)$$

$$(FeH^+)_{ads} + e^- \rightarrow (FeH)_{ads} \quad (13)$$

$$(FeH)_{ads} + H^+ + e^- \rightarrow Fe + H_2 \quad (14)$$

The polarization curves without and with various concentrations of N5MHP in 1 M HCl media are depicted in Fig. 2. Figure 2 shows that both the anodic and branch cathodic reactions were influenced by the addition of N5MHP, which reduced both the cathodic hydrogen evolution and the anodic N80 steel dissolution (Mobin and Rizvi 2017; James and Iroha 2021). This indicates that N5MHP behaved as a mixed-type inhibitor. The electrochemical polarization parameters like corrosion current density (i_{corr}), corrosion potential (E_{corr}), inhibition efficiency (IE_{PDP}, %), anodic branch slope (β_a) and cathodic branch slope (β_c) were deduced by means

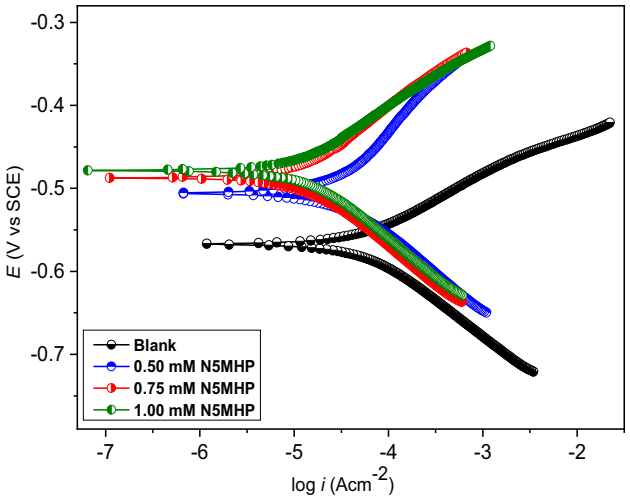

Fig. 2 Potentiodynamic polarization curves of N80 steel in 1 M HCl solutions without and with various concentrations of N5MHP of N5B2HP at 30 °C

of Tafel extrapolation and listed in Table 1. The IE_{PDP} was calculated as follows:

$$IE_{PDP} = \frac{I^0_{corr} - I^i_{corr}}{I^0_{corr}} \times 100 \quad (15)$$

where I^0_{corr} and I^i_{corr} are the corrosion current densities without and with N5MHP inhibitor respectively. The results as shown in Table 1 indicate that the presence of various concentrations of N5MHP cause a significant decrease in the i_{corr} values. The observed decrease of the i_{corr} values was due to the inhibitor adsorption on the N80 steel/HCl interface (Obot et al. 2015; Iroha and Akaranta 2020). Maximum inhibition efficiency was obtained at the concentration of 1.00 mM of N5MHP. Generally, a shift in E_{corr} above 85 mV, categorizes the inhibitor as cathodic or anodic and a shift lower than 85 mV (as seen in this study) suggest that the inhibitor is mixed-type (Olasunkanmi et al. 2017; Abeng et al. 2023; Iroha and Ukpe 2020). The Tafel slopes (β_a and β_c) decrease with an increase in N5MHP concentration, which further suggests the suppression of both cathodic and anodic partial reactions.

Electrochemical impedance measurement

The impedance study was carried out to elucidate the kinetics and characteristics of the metal/solution interface and how N5MHP obstructed the reaction. The Nyquist plots of N80 steel in 1 M HCl medium without and with various concentrations of N5MHP is depicted in Fig. 3. The figure clearly shows a depressed semicircular shape for all the impedance spectra. Slight deviations of the shape from a perfectly circle suggest interfacial impedance frequency dispersion (Da-Rocha et al. 2010; Pavithra et al. 2010). The equivalent circuit used in modeling the N80 steel/HCl solution interface is depicted as an insert in Fig. 3, where R_s denotes solution resistance, R_{ct} stands for charge transfer resistance and CPE is the constant phase element used to replace double layer capacitance (C_{dl}). The CPE impedance is expressed as:

$$Z_{CPE} = \frac{1}{Y_o}(j\omega)^{-n} \quad (16)$$

where Y_0 denotes CPE constant, ω is angular frequency, $j^2 = -1$ is imaginary number and n is the CPE exponent which presents information on the degree of surface inhomogeneity resulting from inhibitor adsorption, surface roughness and formation of porous layer (Abdel-Gaber et al. 2009). The C_{dl} values are computed from CPE utilizing Eq. 17:

$$C_{dl} = Y_0(\omega_{max})^{n-1} \quad (17)$$

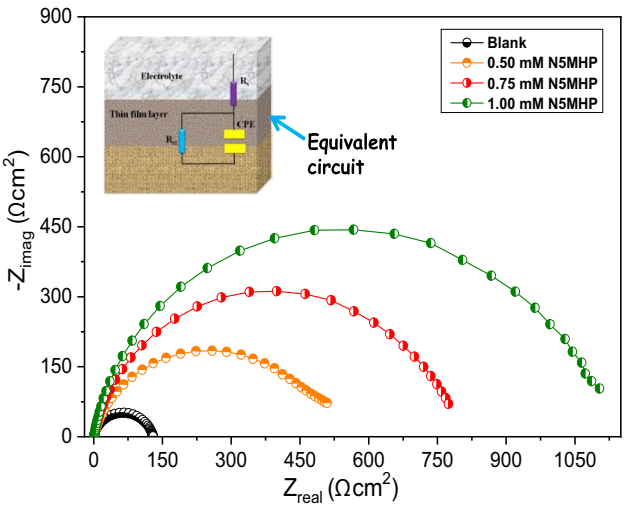

Fig. 3 Nyquist plot of N80 steel in 1 M HCl without and with various concentrations of N5MHP (insert: equivalent circuit)

Table 1 Potentiodynamic polarization data of N80 steel in 1 M HCl without and with various concentrations of N5MHP at 30 °C

Conc. (mM)	i_{corr} (μA cm^{-2})	E_{corr} (mV/SCE)	β_a (mV dec^{-1})	β_c (mV dec^{-1})	η_{PDP}(%)
Blank	796.3	-569.1	117.4	166.9	-
0.50	233.7	-502.8	102.5	142.8	70.7
0.75	139.9	-488.0	113.9	137.2	82.4
1.00	52.6	-477.6	115.8	124.3	93.4

Where, ω_{max} denotes the frequency at which the impedance imaginary part has attain maximum value. The impedance parameters such as R_{ct}, C_{dl} and inhibition efficiency (IE_{EIS}, %), are listed in Table 2. The IE_{EIS} was computed as follows:

$$IE_{EIS} = \frac{R_{ct} - R_{ct}^{0}}{R_{ct}} \times 100 \quad (15)$$

where R_{ct}^{0} and R_{ct} are the charge transfer resistances without and with N5MHP inhibitor respectively. It is obvious that R_{ct} values increase with increasing N5MHP concentrations. This indicates a decrease in corrosion rate in the inhibitor presence and an increase in IE_{EIS}. On the other hand, the C_{dl} values were found to decrease on adding N5MHP inhibitor, which indicates a decrease in local dielectric constant and/or an increase in the electrical double layer thickness, suggesting that N5MHP function by protective layer formation on the N80 steel surface (Ostovari et al. 2009; Iroha et al. 2023a, b).

Weight loss method

Effect of concentration

The variation of weight loss parameters with the concentrations of N5MHP is depicted in Fig. 4. It is observed that N5MHP protected N80 steel corrosion in the HCl solution at all studied concentrations i.e. 0.50 to 1.00 mM, with C_R decreasing with an increase in the inhibitors concentration while the reverse was the case for IE_{WL} %. However, the Schiff base pyridine-2-amine derivative showed maximum protection at 303 K with 1.00 mM concentration. The results in Fig. 1b reveal that N5MHP performed well in protecting the steel surface, achieving an inhibition efficiency of 97.0% at 303 K with 1.0 mM concentration. The corrosion rate on the other hand, decreased from 8.465 mg/cm^2/h to 0.452 mg/cm^2/h in the presence of 1.00 mM N5MHP at 303 K. This observed result is related to increased adsorption of inhibitor species leading to hydrophobic thin film formation on the acid-substrate interface (Iroha et al. 2015).

Impact of temperature

The impact of temperature on N80 steel corrosion behaviour in inhibited and uninhibited test solutions was studied. The observed variation of C_R and IE_{WL}% with temperature ranging from 303 to 323 K are displayed in Table 3. The table reveals that C_R of X60 steel in both inhibited and uninhibited solutions increased with increase in temperature while IE_{WL} % for N5MHP at constant concentration, decreased with temperature rise. This observation could be due to desorption of adsorbed inhibitor species caused by elevated temperature (Fragoza-Mar et al. 2012; Mourya et al. 2016).

Activation and thermodynamic parameters were considered to help in the understanding of the adsorption and inhibition mechanism. The C_R is observed to depend on temperature and this dependency on temperature is expressed

Table 2 Electrochemical impedance parameters for N80 steel in 1 M HCl without and with various concentrations of N5MHP at 30 °C

Conc. (mM)	R_s (Ω cm^2)	R_{ct} (Ω cm^2)	C_{dl} (μF cm^{-2})	n	η_{EIS}(%)
Blank	0.864	123.8	20.67	0.838	-
0.50	0.886	495.2	16.51	0.849	75.0
0.75	0.903	661.0	8.91	0.864	81.3
1.00	0.975	2189.6	3.11	0.882	94.3

Table 3 Variation of C_R and IE_{WL} with temperature without and with 1.00 mM N5MHP in 1 M HCl

	C_R (mgcm^{-2}h^{-1})		IE_{WL}(%)
T (K)	Blank	N5MHP	N5MHP
303	8.465	0.254	97.0
313	12.160	0.746	93.9
323	16.090	1.694	89.5

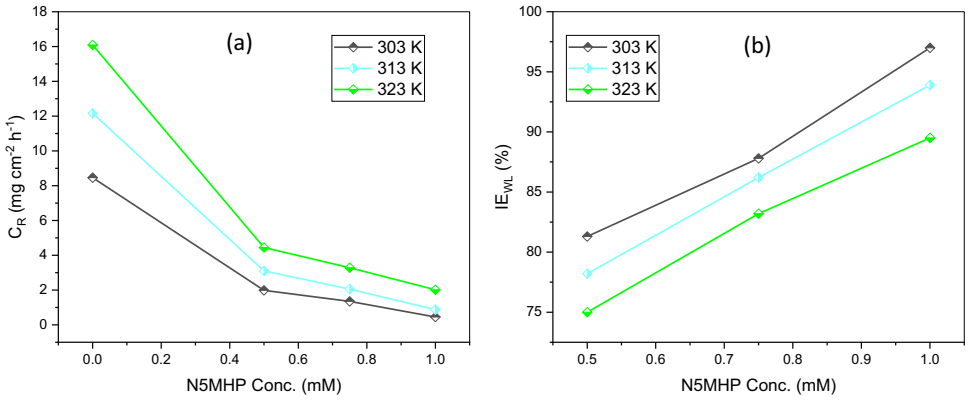

Fig. 4 Variation of **a** C_R and **b** IE_{WL} with N5MHP concentration for N80 steel at different temperatures

utilizing the Arrhenius equation (Verma et al. 2016; Chokor et al. 2022):

$$log\ C_R = \frac{-E_a}{2.303RT} + log\ A \tag{16}$$

Where E_a is denotes activation energ, T is the absolute temperature, R stands for gas constant, and A denotes pre-exponential factor. Plot of $log\ C_R$ against 1/T (Arrhenius plot) for N80 steel dissolution without and with different concentrations of N5MHP is displayed in Fig. 5a. The E_a values deduced from the Arrhenius plot slope are listed in Table 4. The data in Table 4 clearly shows that E_a values in presence of N5MHP were higher when compared with the values without N5MHP. This observation indicates that N5MHP retards the dissolution N80 steel by causing an increase in the energy barrier involved in corrosion (Krishnegowda et al. 2013). An alternative formula for the Arrhenius equation is the Eyring's transition state equation given as:

$$\log\frac{C_R}{T} = \log\left(\frac{R}{Nh}\right) + \left(\frac{\Delta S^*}{2.303R}\right) - \left(\frac{\Delta H^*}{2.303RT}\right) \tag{17}$$

where N is Avogadro's number, h denotes Planck's constant, ΔS^* stands for activation entropy, ΔH^* denotes activation enthalpy. From the slope ($-\Delta H^*/2.303R$) of the plot of log C_R/T against 1/T (Transition state plot) depicted in Fig. 5b, ΔH^* values were computed. The ΔS^* values were deduced from the intercept, [log (R/Nh) + (ΔS^*/2.303R)] of the same plot. These values are listed in Table 4. The positive ΔH^* values obtained shows the endothermic nature of the N80 steel dissolution in the presence of N5MHP. The values ΔS^* in the presence of N5MHP and its absence are both negative with less negative values in the presence of N5MHP. This suggests that the activation complex in the rate determining step denotes association instead of dissolution step, which implies decreased disorderliness on going from reactants to activated complex. The negative ΔS^* values also shows the non-spontaneous nature of the N80 steel dissolution by adding N5MHP (Ikeuba et al. 2015).

Table 4 Activation parameters for the dissolution of N80 steel in the absence and presence of various concentrations of N5MHP.

Conc(mM)	E_a(kJ/mol)	ΔH^*(kJ/mol)	ΔS^*(J/mol/K)
Blank	31.63	27.51	-159.31
0.50	38.19	33.86	-144.64
0.75	42.75	39.01	-138.99
1.00	50.46	42.68	-122.53

Adsorption isotherm

Adsorption isotherm was studied to better understand the interaction between the N80 steel surface and N5MHP in 1 M HCl environment. Among the various adsorption isotherms tested, Langmuir isotherm gave the best fit. The Langmuir isotherm is given as:

$$\frac{C_{inh}}{\theta} = \frac{1}{K_{ads}} + C_{inh} \tag{17}$$

where C_{inh} denotes N5MHP concentration and K_{ads} stands for adsorption equilibrium constant. A plot of C_{inh}/θ against C_{inh} as depicted in Fig. 6, gives a straight line with the values of regression coefficient (R^2) and slope very close to unity suggesting that N5MHP adsorption on the N80 steel surface in test solution obeys the Langmuir adsorption isotherms (Iroha et al. 2012). The K_{ads} is related to the adsorption free energy (ΔG^0_{ads}) as follows:

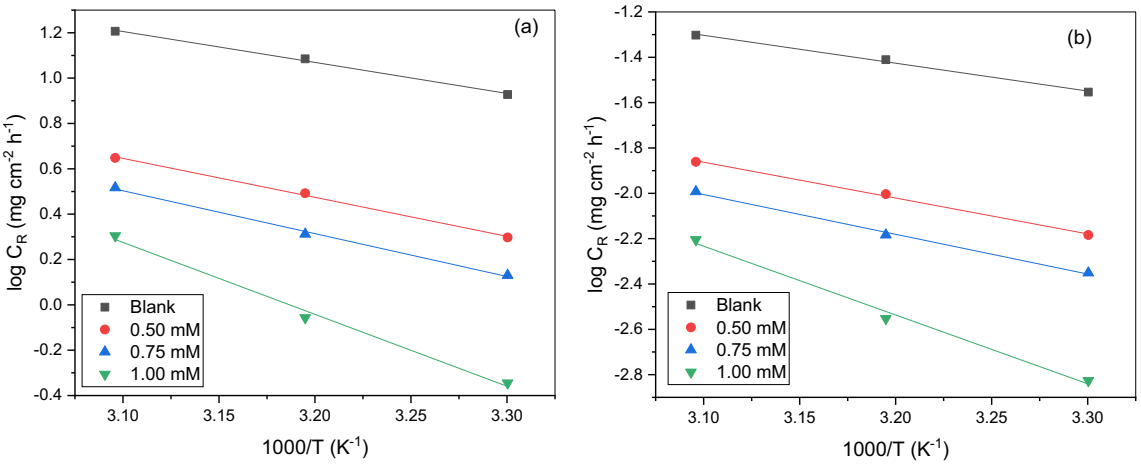

Fig. 5 **a** Arrhenius plots and **b** Transition state plots for N80 steel in the absence and presence of different concentrations of N5MHP

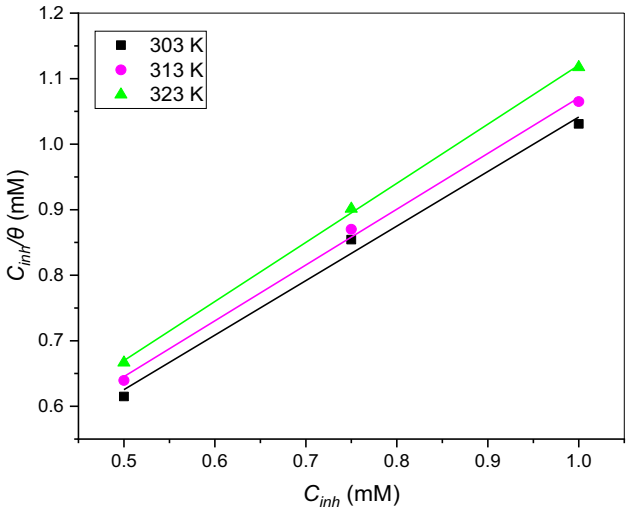

Fig. 6 Langmuir isotherm for the adsorption of N5MHP on N80 steel surface using weight loss method

Table 5 Thermodynamic parameters for the adsorption of N5MHP on N80 steel in 1 M HCl at various temperature

Temp. (K)	R^2	Slope	Intercept	K_{ads} (M^{-1})	ΔG^0_{ads} (kJ/mol)
303	0.9851	0.8318	0.2095	4773	-31.46
313	0.9953	0.8512	0.2198	4550	-32.37
323	0.9988	0.9013	0.2192	4562	-33.41

$$\Delta G^{o}_{ads} = -RT\ln\left(55.5K_{ads}\right) \quad (18)$$

where R denotes the gas constant and T stands for absolute temperature. The value, 55.5 is the molar concentration of water in solution. The computed values of K_{ads} and ΔG^0_{ads} are presented in Table 5. The values of the Langmuir isotherm slopes show deviations from unity expected for ideal an ideal Langmuir isotherm equation. The deviation from 1 could be as a result of interactions between the adsorbed molecules on the X60 steel surface. The observed negative ΔG^0_{ads} values show that the adsorption process is spontaneous. General, ΔG^0_{ads} values of within -20 kJmol^{-1} are associated with physisorption while values more negative than -40 kJmol^{-1} are compatible with chemisorption (Yadav et al. 2015a). The computed ΔG^0_{ads} values for N5MHP are between -31.46 to -33.41 kJmol^{-1} which are within the threshold values for physisorption and chemisorption, suggesting that the adsorption process of N5MHP on N80 steel surface involves both chemical and physical adsorption (Yadav et al. 2015b).

SEM analysis

The surface morphology of uninhibited and inhibited N80 steel samples after immersion period of 6 h are depicted in Fig. 7. The SEM image of the specimen immersed in uninhibited 1 M HCl environment (Fig. 7a) is porous and rough due to aggressive and fast acid corrosion reaction. Moreover, the SEM images of the N80 steel specimen in presence of N5MHP (Fig. 7b) is less damaged, indicating a retardation of the corrosion attack and protective film formation of N5MHP on the steel surface.

Quantum chemical calculation

The frontier molecular orbitals (FMOs) are very important tool in determining the chemical reactivity of the inhibitor adsorbed onto metal surfaces (Daoud et al. 2015). Figure 8 shows graphical representations of the HOMO and LUMO density distribution of N5MHP. The depiction in Fig. 8 shows that the HOMO and LUMO orbitals' sites of distribution are mainly the azomethine group, π-electrons, including the heteroatoms of oxygen and nitrogen. The quantum chemical properties of the neutral and protonated forms of N5MHP are listed in Table 6. The E_{HOMO} values are generally related to the ability of the inhibitor molecules to donate electron to the unoccupied metal surface's d-orbital. Higher values of E_{HOMO} imply

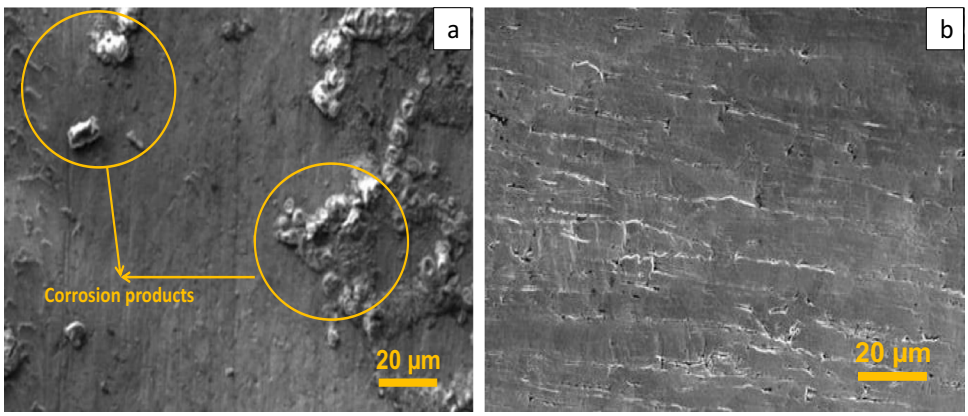

Fig. 7 SEM images for N80 steel **a** exposed to 1 M HCl **b** exposed to 1 M HCl containing 1.00 mM N5MHP.

that the electron donating ability including the inhibition efficiencies of the inhibitor would be high. However, E_{LUMO} values are related to the ability of the inhibitor molecule to accept electron from the metal. Therefore, the electron accepting properties including the inhibition efficiency increases with reduced E_{LUMO} values (Verma et al. 2016). As observed in Table 6, the high E_{HOMO} of neutral N5MHP is stabilized in N5MHP-H^+ (protonated form) which suggests lower electron-donating ability of N5MHP-H^+. The energy band gap (ΔE) relates the stability and chemical reactivity of the inhibitor molecules. Lower values of ΔE facilitate and increase the adsorption of the inhibitor molecule on the metal surface through donor-acceptor process (Boughoues et al. 2020). In the present study, ΔE of N5MHP-H^+ is lower than that of N5MHP, which promotes its adsorption to the N80 steel surface and enhances its efficiency. The hardness (η) and softness (σ) are other properties that are related to molecular reactivity and stability. A hard molecule has higher ΔE between the E_{LUMO} and E_{HOMO} and is related to lower reactivity and inhibition efficiency. On the other hand, a soft molecule has a lower ΔE between the E_{LUMO} and E_{HOMO} and is related to larger reactivity and inhibition efficiency (Mohamed et al. 2021). The fraction of transferred electrons (ΔN) from our study are less than 3.6 for N5MHP and N5MHP-H^+ molecules, suggesting transfer of electrons from the molecules to N80 steel leading to formation of dative bonds. This promotes protective layer formation against corrosion.

Table 6 Calculated quantum chemical parameters for N5MHP and N5MHP-H^+ molecules

Theoretical parameters	N5MHP	N5MHP-H^+
E_{HOMO} (eV)	-4.34	-8.33
E_{LUMO} (eV)	-2.21	-6.85
ΔE ($E_{LUMO} - E_{HOMO}$) (eV)	2.13	1.48
Ionization energy (I)	4.34	8.33
Electron affinity (A)	2.21	6.85
Electronegativity (χ)	3.28	7.59
Global hardness (η)	1.07	0.74
Global softness (σ)	0.93	1.35
Fraction of transferred electrons (ΔN)	1.74	-0.40

Conclusion

The present study has shown that the synthesized N-(5-methoxy-2-hydroxybenzylidene)pyridine-2-amine (N5MHP) can function as an effective corrosion inhibitor for N80 pipeline steel in 1 M HCl solution and the inhibition efficiency increases with increasing concentration of the inhibitor. The corrosion process was inhibited by adsorption of the Schiff base molecules on N80 steel surface leading to the formation of a protective film on the metal/acid solution interface, decreasing the dissolution of the steel. Results from Potentiodynamic polarization showed that the studied inhibitor exhibit mixed-type inhibition activity. The results of the EIS reveal that there is a decrease in the charge transfer resistance in the presence of N5MHP. The impact of temperature on the inhibition performance of N5MHP was investigated using weight loss measurements and the results indicated that the inhibition efficiency of N5MHP decreases with increase in temperature. Adsorption of the studied inhibitor obeys Langmuir adsorption isotherm. The results obtained from EIS, weight loss and polarization techniques are in good agreement. Surface analysis by SEM confirms the adsorption performance of the inhibitor and the development of a protective film on the steel surface. Additionally, the results obtained by the DFT-based quantum chemical calculations supported the experimental findings.

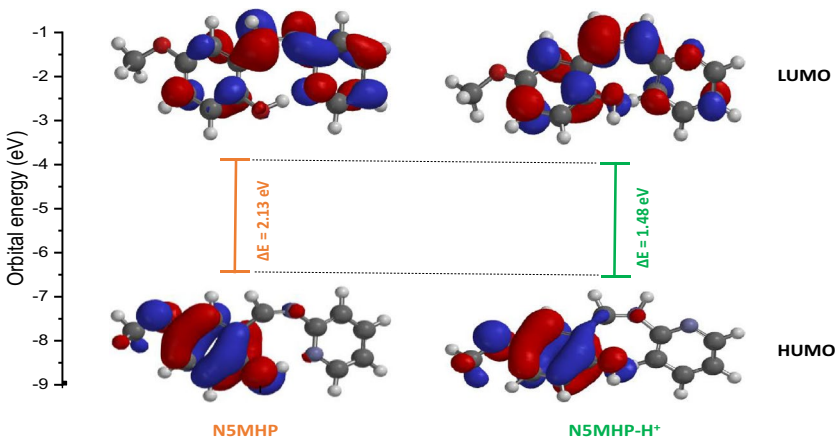

Fig. 8 Frontier molecular orbitals HOMO and LUMO of neutral and protonated N5MHP

Acknowledgements The authors thankfully acknowledge the Tertiary Education Trust Fund (TETFUND), Nigeria for providing financial support under Institution Based Research (IBR) scheme.

Author contributions Nkem B. Iroha: Designed the study, Wrote the first draft of the manuscript, Performed the electrochemical experiments and surface analysis, Cordelia U. Dueke-Eze: Performed the weight loss experiments and DFT, Managed the literature searches, Took part in the manuscript writing. Both authors Wrote, Edited and finalized the manuscript.

Funding This work was funded by TETFUND Institution Based Research Scheme.

Data availability All data generated or analysed during this study are included in this published article.

Declarations

Ethical approval Not applicable.

Competing interests The authors declare that they have no known competing financial interests or personal relationships that could have appeared to influence the work reported in this paper.

References

ASTM G31-72 (2004) Standard practices for laboratory immersion corrosion testing of metals

Abd-Elaal AA, Aiad I, Shaban SM, Tawfik SM, Sayed A (2013) Synthesis and evaluation of some triazole derivatives as corrosion inhibitors and biocides. J Surfact Deterg 17(3):483–449. https://doi.org/10.1007/s11743-013-1547-0

Abdel-Gaber AM, Abd-El-Nabey BA, Saadawy M (2009) The role of acid anion on the inhibition of the acidic corrosion of steel by lupine extract. Corros Sci 51:1038–1042. https://doi.org/10.1016/j.corsci.2009.03.003

Abeng FE, Ita BI, Anadebe VC, Chukwuike VI, Etiowo KM, Nkom PY, Ekerenam OO, Iroha NB, Ikot IJ (2023) Multidimensional insight into the corrosion mitigation of clonazepam drug molecule on mild steel in chloride environment: empirical and computer simulation explorations. Results Eng 17:100924. https://doi.org/10.1016/j.jtice.2015.06.020

Ansari KR, Quraishi MA, Singh A (2015) Pyridine derivatives as corrosion inhibitors for N80 steel in 15% HCl: electrochemical, surface and quantum chemical studies. Measurement 76:136–147. https://doi.org/10.1016/j.measurement.2015.08.028

Anwar S, Khan F, Zhang Y, Caines S (2019) Optimization of zinc-nickel film electrodeposition for better corrosion resistant characteristics. Can J Chem Eng 97:2426–2439. https://doi.org/10.1002/cjce.23521

Anwar S, Khan F, Zhang Y, Caines S (2021) Zn composite corrosion resistance coatings: what works and what does not work? J Loss Prev Process Ind 69:104376. https://doi.org/10.1016/j.jlp.2020.104376

Arrousse N, Salim R, Benhiba F, Mabrouk EH, Abdelaoui A, El Hajjaji F, Warad I, Zarrouk A, Taleb M (2021) Insight into the corrosion inhibition property of two new soluble and non-toxic xanthen-benzoate derivatives. J Mol Liq 338:116610. https://doi.org/10.1016/j.molliq.2021.116610

Boughoues Y, Benamira M, Messaadia L, Bouider N, Abdelaziz S (2020) Experimental and theoretical investigations of four amine derivatives as effective corrosion inhibitors for mild steel in HCl medium. RSC Adv 10:24145–24158. https://doi.org/10.1039/d0ra03560b

Chokor AA, Dueke-Eze CU, Nnanna LA, Iroha NB (2022) Adsorption, electrochemical and theoretical studies on the protective effect of N-(5-bromo-2-hydroxybenzylidene) isonicotinohydrazide on carbon steel corrosion in aggressive acid environment. Saf Extreme Environ 4(1):35–45. https://doi.org/10.1007/s42797-022-00050-8

Cocco MT, Congiu C, Onnis V, Morelli M, Cauli O (2003) Synthesis of ibuprofen heterocyclic amides and investigation of their analgesic and toxicological properties. Eur J Med Chem 38:513–518. https://doi.org/10.1016/s0223-5234(03)00074-6

Daoud D, Douadi T, Hamani H, Chafaa S, Al-Noaimi M (2015) Corrosion inhibition of mild steel by two new Sheterocyclic compounds in 1 M HCl: experimental and computational study. Corros Sci 94:21–37. https://doi.org/10.1016/j.corsci.2015.01.025

Dueke-Eze CU, Fasina TM, Mphahlele MJ (2013) Synthesis, characterization and solvent effects on the electronic absorption spectra of aminopyridine Schiff bases. Asian J Chem 25(15):8505–8508. https://doi.org/10.14233/ajchem.2013.14805

Dueke Eze CU, Madueke NA, Iroha NB, Maduelosi NJ, Nnanna LA, Anadebe VC, Chokor AA (2022) Adsorption and inhibition study of N-(5-methoxy-2-hydroxybenzylidene) isonicotinohydrazide Schiff base on copper corrosion in 3.5% NaCl. Egypt J Pet 31:31–37. https://doi.org/10.1016/j.ejpe.2022.05.001

El Kacimi Y, Azaroua MA, Touir R, Galai M, Alaoui K, Sfaira M, Ebn Touhami M, Kaya S (2017) Corrosion inhibition studies for mild steel in 5.0 M HCl by substituted phenyltetrazole. Euro-Mediterr J Environ Integr 2:1. https://doi.org/10.1007/s41207-016-0011-8

Fragoza-Mar L, Olivares-Xometl O, Domínguez-Aguilar MA, Flores EA, Arellanes-Lozada P, Jimenez-Cruz F (2012) Corrosion inhibitor activity of 1,3-diketonemalonates for mild steel in aqueous hydrochloric acid solution. Corros Sci 61:171–184. https://doi.org/10.1016/j.corsci.2012.04.031

Hamani H, Douadi T, Al-Noaimi M, Issaadi S, Daoud D, Chafaa S (2014) Electrochemical and quantum chemical studies of some azomethine compounds as corrosion inhibitors for mild steel in 1 M hydrochloric acid. Corros Sci 88:234–245. https://doi.org/10.1016/j.corsci.2014.07.044

Hughes TV, Xu G, Wetter SK, Connolly PJ, Emanuel SL, Karnachi P, Pollack SR, Pandey N, Adams M, Moreno-Mazza S, Middleton SA, Greenberger LM (2008) A novel 5-[1,3,4-oxadiazol-2-yl]-N-aryl-4,6-pyrimidine diamine having dual EGFR/HER2 kinase activity: design, synthesis, and biological activity. Bioorg Med Chem Lett 18:4896–4899. https://doi.org/10.1016/j.bmcl.2008.07.057

Ikeuba AI, Ita BI, Okafor PC, Ugi BU, Kporokpo EB (2015) Green corrosion inhibitors for mild steel in H2SO4 solution: comparative study of Flavonoids extracted from Gongronema atifoliunm with crude the extract. Prot Met Phys Chem Surf 51:1043–1049. https://doi.org/10.1134/S2070205115060118

Iroha NB, Akaranta O (2020) Experimental and surface morphological study of corrosion inhibition of N80 carbon steel in HCl stimulated acidizing solution using gum exudate from Terminalia mentaly. SN Appl Sci 2:1514. https://doi.org/10.1007/s42452-020-03296-8

Iroha NB, Akaranta O, James AO (2012) Corrosion inhibition of mild steel in acid media by red peanut skin extract-furfural resin. Adv Appl Sci Res 3(6):3593–3598

Iroha NB, Akaranta O, James AO (2015) Red onion skin extract-formaldehyde resin as corrosion inhibitor for mild steel in hydrochloric acid solution. Int Res J Pure App Chem 6(4):174–181. https://doi.org/10.9734/IRJPAC/2015/9555

Iroha NB, Anadebe VC, Maduelosi NJ, Nnanna LA, Isaiah LC, Dagdag O, Berisha A, Ebenso EE (2023a) Linagliptin drug molecule as corrosion inhibitor for mild steel in 1 M HCl solution: electrochemical, SEM/XPS, DFT and MC/MD simulation approach. Colloids Surf A Physicochem Eng Asp 660:130885. https://doi.org/10.1016/j.colsurfa.2022.130885

Iroha NB, Maduelosi NJ, Nnanna LA (2023b) The impact of tizanidine on E24 carbon steel corrosion inhibition in oilfield acidizing solution: experimental and quantum chemical studies. Emergent Mater 6:137–146. https://doi.org/10.1007/s42247-022-00400-z

Iroha NB, Dueke-Eze CU (2021) Experimental studies on two isonicotinohydrazidebased schiff bases as new and efficient inhibitors for pipeline steel rrosion corrosion in acidic cleaning solution. Chem Afr 4(3):635–646. https://doi.org/10.1007/s42250-021-00252-w

Iroha NB, Nnanna LA, Maduelosi NJ, Anadebe VC, Abeng FE (2022a) Evaluation of the anticorrosion performance of Tamsulosin as corrosion inhibitor for pipeline steel in acidic environment: experimental and theoretical study. J Taibah Univ Sci 16(1):288–299. https://doi.org/10.1080/16583655.2022.2048512

Iroha NB, Dueke-Eze CU, Fasina TM, Anadebe VC, Guo L (2022b) Anticorrosion activity of two new pyridine derivatives in protecting X70 pipeline steel in oil well acidizing fluid: experimental and quantum chemical studies. J Iran Chem Soc 19(6):2331–2346. https://doi.org/10.1007/s13738-021-02450-2

Iroha NB, Dueke-Eze CU, James AO, Fasina TM (2021) Newly synthesized N-(5-nitro-2-hydroxybenzylidene) pyridine-4-amine as a high-potential inhibitor for pipeline steel corrosion in hydrochloric acid medium. Egypt J Pet 30:55–61. https://doi.org/10.1016/j.ejpe.2021.02.003

Iroha NB, James AO (2019) Adsorption behavior of pharmaceutically active dexketoprofen as sustainable corrosion inhibitor for API X80 carbon steel in acidic medium. World News Nat Sci 27:22–37

Iroha NB, Nnanna LA (2021) Tranexamic acid as novel corrosion inhibitor for X60 Steel in oil well acidizing fluids: surface morphology, gravimetric and electrochemical studies. Prog Color Color Coat 14:1–11. https://doi.org/10.30509/PCCC.2021.81663

Iroha NB, Oguzie EE, Onuoha GN, Onuchukwu AI (2005) Inhibition of mild steel corrosion in acidic solution by derivatives of diphenyl glyoxal. Proceedings of the 16th International Corrosion Congress held in Beijing, China

Iroha NB, Ukpe RA (2020) Investigation of the inhibition of the corrosion of carbon steel in solution of HCl by Glimepiride. Commun Phys Sci 5:246–256

James AO, Iroha NB (2021) New green inhibitor of Olax subscorpioidea root for J55 carbon steel corrosion in 15% HCl: theoretical, electrochemical, and surface morphological investigation. Emergent Mater 5:1119–1131. https://doi.org/10.1007/s42247-021-00161-1

Kousar K, Walczak MS, Ljungdahl T, Wetzel A, Oskarsson H, Restuccia P, Ahmad EA, Harrison NM, Lindsay R (2021) Corrosion inhibition of carbon steel in hydrochloric acid: elucidating the performance of an imidazoline-based surfactant. Corros Sci 180:109195. https://doi.org/10.1016/j.corsci.2020.109195

Krishnegowda PM, Venkatesha VT, Krishnegowda PKM, Shivayogiraju SB (2013) Acalypha torta leaf extract as green corrosion inhibitor for mild steel in hydrochloric acid solution. Ind Eng Chem Res 52:722–728. https://doi.org/10.1021/IE3018862

Maduelosi NJ, Iroha NB (2020) Insight into the adsorption and inhibitive effect of spironolactone drug on C38 carbon steel corrosion in hydrochloric acid environment. J Bio- Tribo-Corrosion 7:6. https://doi.org/10.1007/s40735-020-00441-z

Mobin M, Rizvi M (2017) Polysaccharide from Plantago as a green corrosion inhibitor for carbon steel in 1 M HCl solution. Carbohydr Polym 160:172–183. https://doi.org/10.1016/j.carbpol.2016.12.056

Mohamed EA, Hashem HE, Azmy EM, Negm NA, Farag AA (2021) Synthesis, structural analysis, and inhibition approach of novel eco-friendly chalcone derivatives on API X65 steel corrosion in acidic media assessment with DFT & MD studies. Environ Technol Innov 24:101966. https://doi.org/10.1016/j.eti.2021.101966

Mourya P, Singh P, Rastogi RB, Singh MM (2016) Inhibition of mild steel corrosion by 1, 4, 6-trimethyl-2-oxo-1, 2-dihydropyridine-3-carbonitrile and synergistic effect of halide ion in 0.5 M H_2SO_4 Appl Surf Sci 380:141–150. https://doi.org/10.1016/j.apsusc.2016.01.263

Njoku DI, Okafor PC, Lgaz H, Uwakwe KJ, Oguzie EE, Li Y (2021) Outstanding anticorrosion and adsorption properties of 2-amino-6-methoxybenzothiazole on Q235 and X70 carbon steels: Effect of time, XPS, electrochemical and theoretical considerations. J Mol Liq 324:114663. https://doi.org/10.1016/j.molliq.2020.114663

Obot IB, Madhankumar A, Umoren SA, Gasem ZM (2015) Surface protection of mild steel using benzimidazole derivatives: experimental and theoretical approach. J Adhes Sci Technol. https://doi.org/10.1080/01694243.2015.1058544

Okey NC, Obasi NL, Ejikeme PM, Ndinteh DT, Ramasami P, Sherif EM, Akpan ED, Ebenso EE (2020) Evaluation of some amino benzoic acid and 4-aminoantipyrine derived Schiff bases as corrosion inhibitors for mild steel in acidic medium: synthesis, experimental and computational studies. J Mol Liq 315:113773. https://doi.org/10.1016/j.molliq.2020.113773

Olasunkanmi LO, Sebona MF, Ebenso EE (2017) Influence of 6-phenyl-3(2H)-pyridazinone and 3-chloro-6-phenylpyrazine on mild steel corrosion in 0.5 M HCl medium: experimental and theoretical studies. J Mol Struct 1149:549–559. https://doi.org/10.1016/j.molstruc.2017.08.018

Ostovari A, Hoseinieh SM, Peikari M, Shadizadeh SR, Hashemi SJ (2009) Corrosion inhibition of mild steel in 1 M HCl solution by henna extract: a comparative study of the inhibition by henna and its constituents (lawsone, gallic acid, α-d-Glucose and tannic acid). Corros Sci 51:1935–1949. https://doi.org/10.1016/j.corsci.2009.05.024

Pavithra MK, Venkatesha TV, Vathsala K, Nayana KO (2010) Synergistic effect of halide ions on improving corrosion inhibition behaviour of benzisothiozole-3-piperizine hydrochloride on mild steel in 0.5 M H2SO4 medium. Corros Sci 52:3811–3819. https://doi.org/10.1016/j.corsci.2010.07.034

Poojary NG, Kumari P, Rao SA (2021) 4-Hydroxyl-N0-[(3-Hydroxy-4-Methoxyphenyl) Methylidene] Benzohydrazide] as corrosion inhibitor for carbon steel in dilute H_2SO_4 J Fail Anal Prev 21:1264–1273. https://doi.org/10.1007/s11668-021-01166-y

Rocha JC, Gomes JACP, D'Elia E (2010) Corrosion inhibition of carbon steel in hydrochloric acid solution by fruit peel aqueous extracts. Corros Sci 52:2341–2348. https://doi.org/10.1016/j.corsci.2010.03.033

Verma C, Quraishi MA, Singh A (2016) A thermodynamical, electrochemical, theoretical and surface investigation of diheteroaryl thioethers as effective corrosion inhibitors for mild steel in 1 M HCl. J Taiwan Inst Chem Eng 58:127–140. https://doi.org/10.1016/j.jtice.2015.06.020

Xia G, Jiang X, Zhou L, Liao Y, Duan M, Wang H, Pu Q, Zhou J (2015) Synergic effect of methyl acrylate and N-cetylpyridinium bromide in N-cetyl-3-(2-methoxycarbonylvinyl) pyridinium bromide molecule for X70 steel protection. Corros Sci 94:224–236. https://doi.org/10.1016/j.corsci.2015.02.005

Yadav M, Sinha RR, Kumar S, Sarkar TK (2015a) Corrosion inhibition effect of spiropyrimidinethiones on mild steel in 15% HCl solution: insight from electrochemical and quantum studies. RSC Adv 5:70832–70848. https://doi.org/10.1039/C5RA14406J

Yadav M, Sinha RR, Sarkar TK, Tiwari N (2015b) Corrosion inhibition effect of pyrazole derivatives on mild steel in hydrochloric acid solution. J Adhes Sci Technol. https://doi.org/10.1080/01694243.2015.1040979

Yurt A, Duran B, Dal H (2014) An experimental and theoretical investigation on adsorption properties of some diphenolic Schiff bases as corrosion inhibitors at acidic solution/mild steel interface. Arab J Chem 7:732–740. https://doi.org/10.1016/j.arabjc.2010.12.010

Zhang K, Xu B, Yang W, Yin X, Liu Y, Chen Y (2015) Halogen-substituted imidazoline derivatives as corrosion inhibitors for mild steel in hydrochloric acid solution. Corros Sci 90:284–295. https://doi.org/10.1016/j.corsci.2014.10.032

Zhang W, Zhang Z, Li W, Huang X, Ruan L, Wu L (2019) Synergistic effect of phytic acid and benzyltrimethyl ammonium bromide on corrosion inhibition of carbon steel in 0.5 M HCl. Int J Electrochem Sci 14:7348–7362. https://doi.org/10.20964/2019.08.30